3D Elastic FWI for Land Seismic Data: A Graph Space OT Approach

W. HE[1,2]*, R. Brossier[1], L. Metivier[1,3]

[1] University Grenoble Alpes, ISTerre; [2] Aramco Asia; [3] University Grenoble Alpes, CNRS, LJK

Summary

Integrating surface wave information is challenging for land seismic full waveform inversion. Cycle-skipping of surface waves can easily occur due to their highly dispersive and oscillating properties. While this issue can be mitigated using wider basin objective functions, a more severe difficulty is related to the unbalanced amplitude distribution between surface waves and body waves. The energetic surface waves dominate the objective function and drive the inversion to update only the shallow structure. The contribution from body waves is masked and the deep structures are not recovered. In a recent study, we have shown how an optimal-transport based function can help mitigating this issue, providing naturally a better balance between events (KR-OT). Here, we apply a newly introduced OT based misfit function, relying on a graph space approach (GS-OT), in this framework of elastic FWI for land data. GS-OT better handles cycle skipping than KR-OT. We show here that it also helps to balance the amplitude of seismic events. We design a practical workflow based on the GS-OT misfit function, coupled with an on-the-fly source estimation wavelet and a Gaussian-time window strategy. The method is applied to a synthetic case study from the SEAM II Foothill model.

Introduction

Full waveform inversion (FWI) reconstructs the subsurface structure by fitting the synthetics to the observed seismic data. How to interpret surface waves, and more importantly, how to reconstruct deep structures in the presence of surface waves are two challenging issues.

Surface waves are energetic but shallow penetrating. The information carried by surface waves about the near-surface complexities is accumulated and mixed along the source-receiver path in the shallow depth. Surface waves can easily cycle-skip being highly dispersive and oscillating. Yet, the challenge is not only about the cycle-skipping issue, but also the unbalanced amplitude distribution between surface and body waves. When the entire seismograms are incorporated to the objective function, the surface waves dominate the inversion and the contribution from body waves becomes negligible. At the end, only the very shallow depth is reconstructed. Adopting an envelope based objective function (Borisov et al., 2016) or FK domain objective function (Masoni et al., 2013; Pérez Solano et al., 2014) reduces the oscillation of surface waves, therefore mitigates the cycle-skipping issue. However, besides the loss of resolution induced by these objective functions, the amplitude balancing problem is not solved. Consequently, deep structures are not recovered.

In a recent study (He et al., 2019), we have illustrated how a specific OT function (Kantorovich-Rubinstein OT, KR-OT in the following), coupled with a Gaussian-time windowing strategy, helps balancing the amplitudes of different types of events, suggesting that the high amplitudes of surface waves will have less impact into the gradient build-up. However, KR-OT still suffers from cycle skipping if too large time shifts are considered. A graph space OT method has been recently introduced in FWI to overcome the limitations of KR-OT with respect to cycle skipping for large time shifts (Métivier et al., 2019). This prompts us to investigate GS-OT in the frame of elastic FWI for land data. Our aim is to design a practical workflow applicable to real data. We consider a spectral element method to accurately simulate seismic wave propagation in presence of varying topography, using the code SEM46 (Trinh et al., 2019). To better handle the bias due to potential errors in source wavelet estimation, we update them on the fly along with velocity models at each iteration (Plessix and Cao, 2011; He et al., 2018).

Methodology: Optimal transport function for event balancing

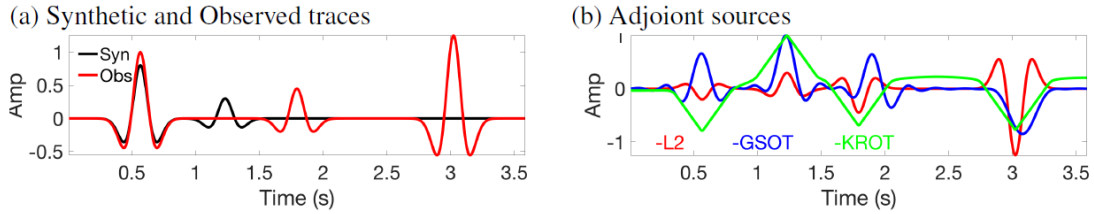

Figure 1: OT (KR, GS) balances events.

The GS-OT strategy is based on a trace-by-trace comparison. Each trace is considered as a point cloud in a 2D space (discrete graph). For the discretized synthetic (ti; pi) and observed trace (t j;dj), the GS-OT distance is defined as finding the permutation s which minimizes

$$h(\mathrm{p}, d) = \min_{\sigma} \sum_{i=1}^{N} \left(t_i - t_{\sigma(i)}\right)^2 + \left(\frac{\tau}{A}\right)^2 \left(p_i - d_{\sigma(i)}\right)^2, \qquad (1)$$

where σ ranges over all the possible permutations of (1;2; :::;N). τ is user-defined parameter, which should be set as the maximum estimated time-shift between synthetics and observed data. A is the maximum amplitude range for each pair of seismic trace. An optimal permutation σ^* can be solved efficiently by the auction algorithm (Bertsekas and Castanon, 1989). The corresponding adjoint source s_i at time t_i is then given by

$$s_i = 2\left(\frac{\tau}{A}\right)^2 \left(p_i - d_{\sigma^*(i)}\right)^2, \tag{2}$$

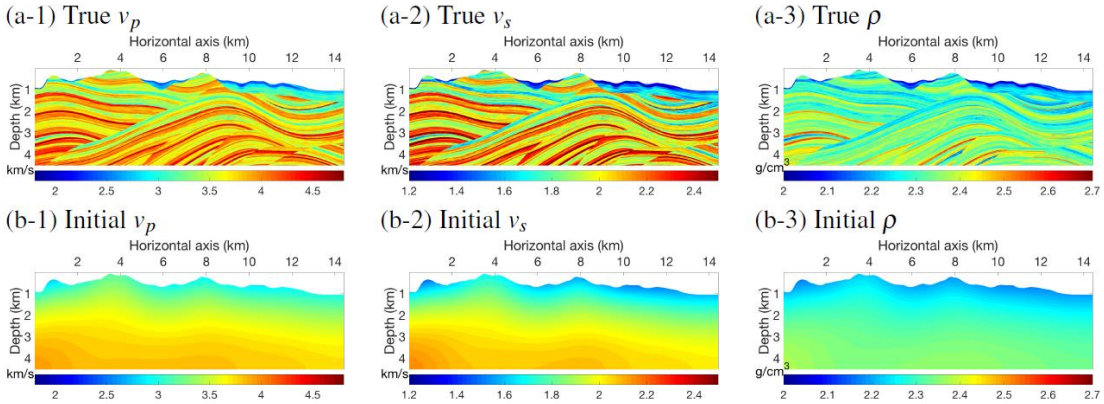

Figure 2: True model (top row) and initial model (bottom row) from the SEAM II Foothill model. During the inversion the density is fixed to the initial value, VP and VS are simultaneously updated.

Equation 1 and 2 apply to each seismic trace. The complete misfit function over the acquisition built by N_r receivers and N_s sources writes

$$f = \sum_{s=1}^{N_s} \sum_{r=1}^{N_r} w_{s,r} h_{s,r}\left(p_{s,r}[m], d_{s,r}\right), \tag{3}$$

where $[m]$ indicates the dependency of synthetic data $p_{s,r}$ on model parameters m. the weight $w_{s,r}$ has been introduced for flexibility. In the following, $w_{s,r}$ is used either based on the energy norm $w_{s,r} = \sum_i^N d_i^2$ of the observations in order to preserve the natural amplitude decay over distances, either as $w_{s,r}$=1 in order to give the same weight to each seismic trace.

In Figure 1, we generate an observed trace and a synthetic trace with 3 Hz Ricker wavelets by mimicking the realistic situation of misaligned and missing events (Δt =7 m, 512 sampling points). The adjoint sources of L^2, KR-OT and GS-OT in Figure 1 reveal that both KR-OT and GS-OT balance the amplitude distribution. This is a good property for land seismic FWI (He et al., 2019).

SEAM model 3D synthetic inversion

Experimental setup

The true model shown in Figure 2 is extracted from 3D SEAM II Foothill model. To simulate the geological process, layered structures are twisted and displaced; also low velocity alluvial zones are padded at the surface. We smooth the true model to remove the layered structures and the near-surface complexity, and take it as initial model (Figure 2). During the inversion, the density is fixed to the smooth initial value to mimic a realistic situation, VP and VS are updated simultaneously. The observed data corresponds to a flat-spectrum response: we do the forward simulation in the true model with a 3 Hz Ricker wavelet, then we deconvolve the data with the same Ricker wavelet. Time interval is Δt = 0.6ms, and total recording time is around 4.8s. We use 16 sources (vertical force, inter-source distance is 900 m), and 720 mono-component geophones (vertical velocity, inter-receiver distance is 20 m).

For the inversion, we use the same mesh and same time increment. In Figure 3 (a), we show the observed data in the first frequency band [1.5, 2.5] Hz. The body waves are hardly visibly despite the use of a strong clip to display the seismogram. Therefore, we normalize all the traces before comparing with the initial synthetics in Figure 3 (b). In the following inversions, a Bessel filter (Trinh et al., 2017) is used to smooth the gradient, the filter length being adapted depending on the local wavelength. Model parameters VP and VS are simultaneously updated using the *l-BFGS* algorithm (Nocedal, 1980; Métivier

and Brossier, 2016).

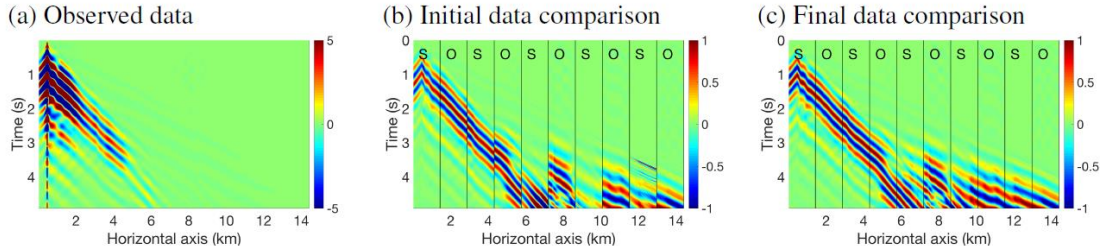

Figure 3: Observed data are shown with its natural amplitude. Data comparison is shown with normalized amplitude. S is synthetic data, O is observed data.

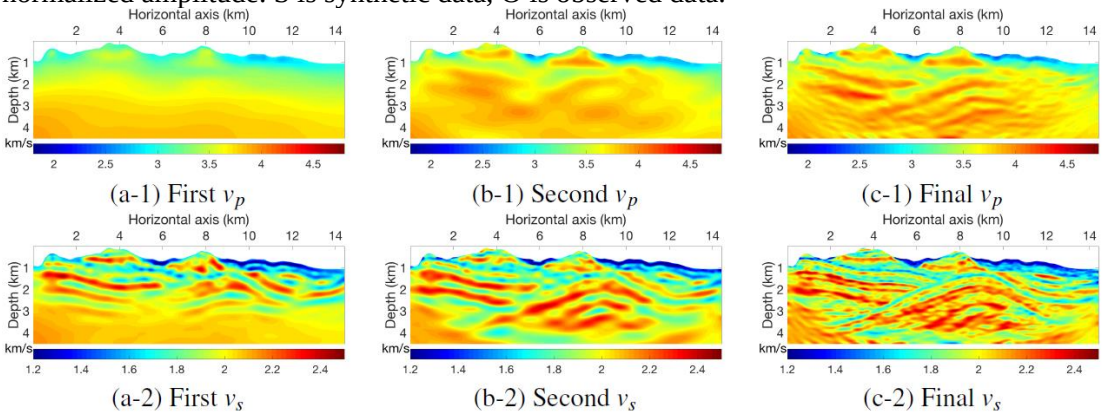

Figure 4: In the first step (top row), surface waves contribute to the inversion. In the second step (second row), body waves contribute to deep reconstruction. In the second frequency band (third row), the final model reveals fine details.

FWI workflow

The first frequency band is [1.5, 2.5] Hz. In the first step, we apply our GS-OT based strategy on the entire seismograms. In this first step, we apply $w_{s,r} = \sum_i^N d_i^2$ in GS-OT (Equation 3) and choose τ =0.2 s. A second step is designed to enhance the contribution from body waves. Then we apply a Gaussian time window roughly around the early body waves (for each seismic trace, the arrival time t is approximated as t=0.6 s+0.3 Δ_{sr} where Δ_{sr} is offset in km). The width of Gaussian window is determined by the standard variation 0.96s (0.2 times of the whole recording time). To further enhance the role of the body waves, we apply $w_{s,r}$=1 to normalize the energy over traces. After the first frequency stage, we enlarge the frequency band to [1.5, 6.5] Hz. We repeat the two-step inversion strategy with $w_{s,r}$=1 in these two steps and decrease τ to 0.1 s.

FWI results

After the first step of the first frequency band, the surface waves are well fitted, but not the body waves (figures not shown); Figure 4 (a-1) and (a-2) show the inverted VP and VS respectively. VS is recovered down to 3 km, while VP is almost not updated. After the second step in the first frequency band, both of the body waves and surface waves are correctly predicted (Figure 3 (c)). The body waves contribute to the model reconstruction at depth, (see inverted models in Figure 4 (b-1) and (b-2)). Both VP and VS are updated significantly.

Moving to the second frequency band, more events including scattered surface waves come out. Following the same two-step workflow, the mismatched body and surface waves are correctly predicted. The final models shown in Figure 4 (c-1) and (c-2) reveal high resolution details, especially for VS.

Conclusion

Our FWI workflow based on the use of GS-OT and on-the-fly wavelet estimation, combined with a two steps process using a Gaussian time-window, seems to provide satisfactory result for a challenging 3D elastic synthetic case study based on the SEAM II Foothill model. Comparisons with the use of KR-OT and L^2 misfit function (not shown here) reveal that the inversion would stop, in this case, after the first step in the first frequency band, indicating probable cycle skipping issues.

These relatively good results obtained with a rather sparse acquisition (16 sources) prompt us to investigate the interest of this workflow on real data. We have started to work on a real dataset acquired in a mountainous area of south China. The preliminary inversion seems consistent with an independent EM survey.

Acknowledgments

This study was partially funded by the SEISCOPE consortium (https://seiscope2.osug.fr), sponsored by AKERBP, CGG, CHEVRON, EQUINOR, EXXON-MOBIL, JGI, PETROBRAS, SCHLUMBERGER, SHELL, SINOPEC and TOTAL. This study was granted access to the HPC resources of CIMENT infrastructure (https://ciment.ujf-grenoble.fr) and CINES/IDRIS/TGCC under the allocation 046091 made by GENCI.

References

Bertsekas, D.P. and Castanon, D. [1989] The auction algorithm for the transportation problem. Annals of Operations Research, 20(1), 67–96.

Borisov, D., Modrak, R., Rusmanugroho, H., Yuan, Y., Simons, F., Tromp, J. and Gao, F. [2016] Spectral-element based 3D elastic full-waveform inversion of surface waves in the presence of complex topography using an envelope-based misfit function. In: SEG Technical Program Expanded Abstracts 2016.

He, W., Brossier, R., Métivier, L. and Plessix, R.É. [2019] Land seismic multi-parameter full waveform inversion in elastic VTI media by simultaneously interpreting body waves and surface waves with an optimal transport based objective function. Geophysical Journal International, 219(3), 1970–1988.

He,W., Brossier, R., Métivier, L. and Virieux, J. [2018] A practical workflow of full waveform inversion to process land seismic data: Synthetic study. In: Expanded Abstracts, 80th Annual EAGE Meeting (Copenhagen).

Masoni, I., Brossier, R., Virieux, J. and Boelle, J. [2013] Alternative Misfit Functions for FWI Applied to Surface Waves. In: EAGE Technical Program Expanded Abstracts 2013, EAGE, Th P10 13.

Métivier, L. and Brossier, R. [2016] The SEISCOPE optimization toolbox: A large-scale nonlinear optimization library based on reverse communication. Geophysics, 81(2), F11–F25.

Métivier, L., Brossier, R., Mérigot, Q. and Oudet, E. [2019] A graph space optimal transport distance asa generalization of L_p distances: application to a seismic imaging inverse problem. Inverse Problems, 35(8), 085001.

Nocedal, J. [1980] Updating Quasi-Newton Matrices With Limited Storage. Mathematics of Computation, 35(151), 773–782.

Pérez Solano, C., Donno, D. and Chauris, H. [2014] Alternative waveform inversion for surface wave analysis in 2-D media. Geophysical Journal international, 198, 1359–1372.

Plessix, R.E. and Cao, Q. [2011] A parametrization study for surface seismic full waveform inversion in an acoustic vertical transversely isotropic medium. Geophysical Journal International, 185, 539–556.

Trinh, P.T., Brossier, R., Métivier, L., Tavard, L. and Virieux, J. [2019] Efficient 3D time-domain elastic and viscoelastic Full Waveform Inversion using a spectral-element method on flexible Cartesian-based mesh. Geophysics, 84(1), R75–R97.

Trinh, P.T., Brossier, R., Métivier, L., Virieux, J. and Wellington, P. [2017] Bessel smoothing filter for spectral element mesh. Geophysical Journal International, 209(3), 1489–1512.